A Calorimeter Coupled with a Magnetic Spectrometer for the Detection of Primary Cosmic Antiprotons.

G. Basini, A. Morselli, M. Occhigrossi, M. Ricci and P. Spillantini

Laboratori Nazionali INFN - Frascati (Roma)

F. Bongiorno

Laboratori Nazionali INFN - Frascati (Roma)
Dipartimento di Metodi e Modelli matematici dell'Università «La Sapienza» - Roma

P. Picozza

Dipartimento di Fisica dell'Università di Tor Vergata - Roma
Laboratori Nazionali INFN - Frascati (Roma)

A. Codino and M. Menichelli

INFN and Dipartimento di Fisica dell'Università - Perugia

S. Bartalucci

CERN - Geneve
Laboratori Nazionali INFN - Frascati (Roma)

Summary. — A tracking calorimeter made of 3200 brass streamer tubes together with 3200 pick-up strips has been built to complement a magnetic spectrometer in order to detect cosmic antiprotons in space. The characteristics of such a calorimeter, the results of a preliminary test of a prototype as well as the properties of the whole apparatus are presented. The apparatus, designed to operate on a balloon at an altitude of about 40 km, can be considered as a second generation detector, capable in principle to solve the problem of the presence of low energy ($\leqslant 1\,\text{GeV}/c$) antiprotons in the cosmic rays which is still open because of the disagreement between the existent experimental data.

PACS 94.40 – Cosmic rays.
PACS 29.40 – Radiation detectors.

1. – Perspectives of antiproton research.

In recent years, the progress in particle detection (e.g., superconducting magnets, compact calorimeters, high-resolution time-of-flight counters) and in space transportation systems has made it possible to start a systematic search for antiparticles in cosmic rays and to verify the present several theories and hypotheses.

This search has for long time been precluded because of the difficulty to transport the heavy traditional detectors in space and the impossibility for earth-based apparata to detect antimatter particles which do not survive the interaction with the atmosphere.

The problem of the primary cosmic antiproton abundance is one of the most puzzling in astrophysics and cosmology. In fact, it seems that there is evidence ([1-3]) of an excess of antiprotons in cosmic rays that cannot be explained with a secondary production via the process $p + p \rightarrow p + \bar{p} +$ anything, following the standard cosmic-ray propagation models ([4]) which compute the expected $\bar{p}$ flux starting from the proton flux, the antiproton production cross-sections and the amount of traversed matter. Slight modifications of these models are unable to explain the observed excess, so that more radical and exotic solutions have been investigated: among them, neutron oscillations ([5]), evaporation of primordial black holes ([6,7]) photino pair annihilation ([8,9]) and the generation of extragalactic antiprotons in antigalaxies in a baryon-antibaryon symmetric Universe ([6,10,11]).

On the other hand, recent data ([12]) from 1987 balloon flight campaign show no excess of antiprotons in the low-energy region over the current prediction.

([1]) R. L. GOLDEN, S. HORAN, B. G. MAUGER, G. D. BADHWAR, J. L. LACY, S. A. STEPHENS, R. R. DANIEL and J. E. ZIPSE: Phys. Rev. Lett., 43, 1196 (1979).
([2]) E. A. BOGOLOMOV, G. Y. VASILYEV, S. YU. KRUT'KOV, N. D. LUBYANAYA, V. A. ROMANOV, S. V. STEPANOV and M. S. SHULAKOVA: Proceedings of the XX International Cosmic Ray Conference, Vol. 2 (Moscow, 1987), p. 72.
([3]) A. BUFFINGTON, S. M. SCHINDLER and C. R. PENNYPACKER: Astrophys. J., 248, 1179 (1981).
([4]) T. K. GAISSER and R. H. MAURER: Phys. Rev. Lett., 30, 1264 (1973).
([5]) C. SIVARAM and V. KRISHAN: Nature, 299, 427 (1982).
([6]) P. KIRALY, C. SZABELSZKI, J. WDOWCZYK and A. W. WOLFENDALE: Nature, 293, 120 (1981).
([7]) M. S. TURNER: Nature, 297, 379 (1982).
([8]) J. SILK and M. SREDNICKI: Phys. Rev. Lett., 53, 624 (1984).
([9]) F. W. STECKER, S. RUDAZ and T. F. WALSH: Phys. Rev. Lett., 55, 2622 (1985).
([10]) F. W. STECKER, R. J. PROTHEROE and D. KAZANAS: Astrophys. Space Sci., 96, 171 (1983).
([11]) S. A. STEPHENS: Proceedings of the XVIII International Cosmic Ray Conference, Vol. 9 (Bangalore, 1983), p. 167.
([12]) S. AHLEN, S. BARWICK, J. J. BEATTY, C. R. BOWER, G. GERBIER, R. M. HEINZ, D. LOWDER, S. MCKEE, S. MUFSON, J. A. MUSSER, P. B. PRICE, M. H. SALAMON, G. TARLE', A. TOMASCH and B. ZHOU: Phys. Rev. Lett., 61, 145 (1988). Other data have been
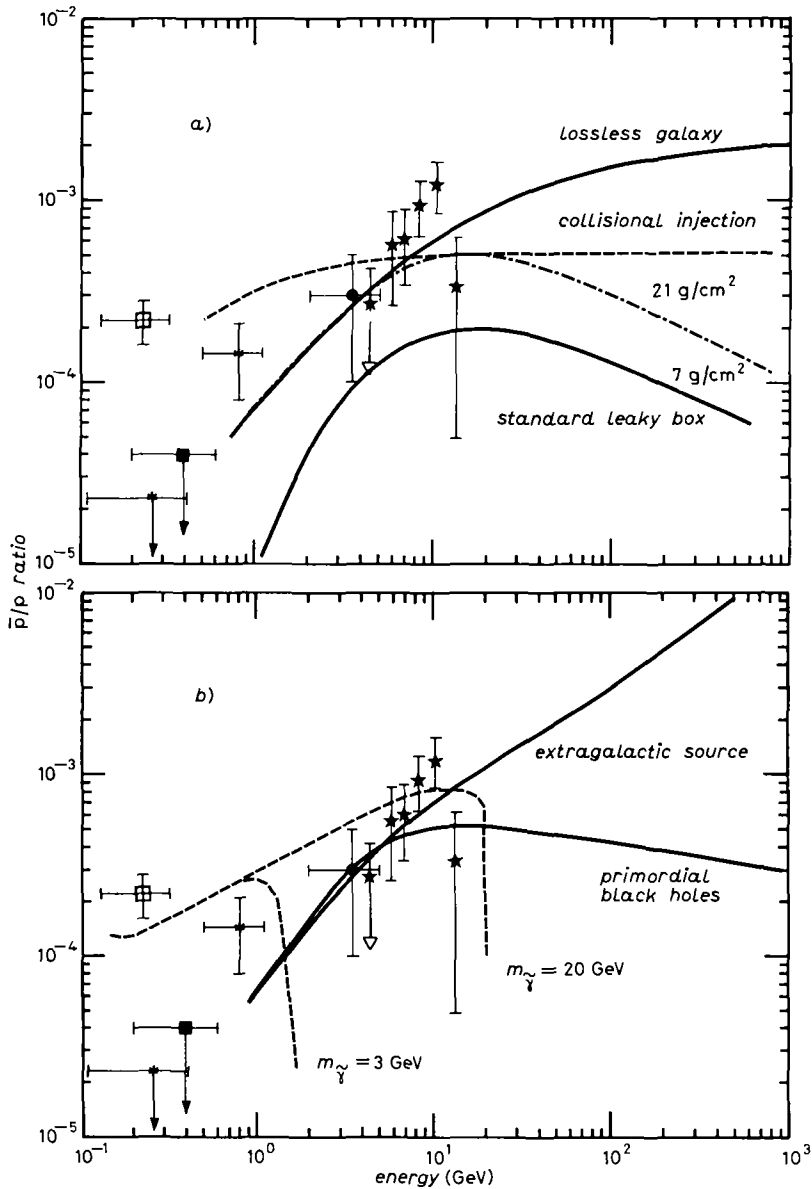
Fig. 1. – The experimental points (see legenda below) are shown compared with the different models for the $\bar{p}/p$ ratio: cosmic-ray models, shown in fig. 1a), cover the hypotheses of «lossless galaxy» [13], production in the early dense phase of a supernova explosion (collisional injection curve) [14,15] and the standard leak box model [16] with a traversed material density of 7 g/cm² and 21 g/cm²; more exotic models, as described in the text are shown in fig. 1b) (see ref. [6-11]). A higher statistics in the measurement of the $\bar{p}$ will clearly lead to discriminate among the different models. Legenda for the experimental points: □ ref. [3]; ● ref. [2]; ★ ref. [17]; ■ Ahlen et al., ref. [12]; ✶ Golden et al., ref. [12].

It is difficult to select between these last results and the previous ones, because of the poor statistics (the quoted measurements collected together about 40 antiprotons) and because no one of the performed experiment (one without magnet, one without tracking calorimeter, one very small) was so significantly better than the others, to lead to a clear conclusion. The present situation including the theoretical models and the experimental data (or upper limits) is shown in fig. 1.

A second generation experiment with an upgraded apparatus, composed of a tracking calorimeter, a magnetic spectrometer using a superconducting magnet, with time-of-flight determination and good geometrical acceptance, should be able, for its completeness, to measure with sufficient statistics the shape of the p̄ spectrum and to discriminate both between theoretical models and between data.

2. – The tracking calorimeter for the antiproton signature.

In order to solve the ambiguities in antiproton detection, we decided to build a calorimeter which provides, together with an energy measurement, also a precise reconstruction of an annihilation vertex and of the tracks coming out from this vertex.

An antiproton annihilation at rest shows a characteristic pattern, the annihilation star, in which the tracks are coming out from a vertex with an average isotropic configuration due to momentum conservation. If the antiproton annihilation takes place in flight secondary particles are boosted forward.

Therefore, an energy deposit greater than the kinetic energy of the incoming particle (the p̄ annihilation gives the contribution of two proton masses to the total energy) and a simultaneous annihilation star configuration are clear p̄ signatures, especially for low-momentum incoming particles. Moreover, in the real flight condition (at an altitude of ~ 40 km), only muons are an important source of negative background, and are easily identified and rejected having a

presented by R. L. GOLDEN at the *VI Course of the International School of Cosmic Ray Astrophysics at Erice, Italy* in April 1988, and are in course of publication.

(13) B. PETERS and N. J. WESTERGAARD: *Astrophys. Space Sci.*, 48, 21 (1977).

(14) G. E. MORAAL and W. I. AXFORD: *Astron. Astrophys.*, 125, 204 (1983).

(15) B. G. MAUGER and A. STEPHENS: *Proceedings of the XVIII International Cosmic Ray Conference*, Vol. 2 (Bangalore, 1983), p. 95.

(16) F. W. STECKER, R. J. PROTHEROE and D. KAZANAS: *Proceedings of the XVII International Cosmic Ray Conference*, Vol. 9 (Paris, 1981), p. 211.

(17) R. L. GOLDEN, B. G. MAUGER, S. NUNN and S. HORAN: *Astrophys. Lett.*, 24, 75 (1984).

different topology from the antiproton annihilation signature (the muon just gives a straight track in the calorimeter).
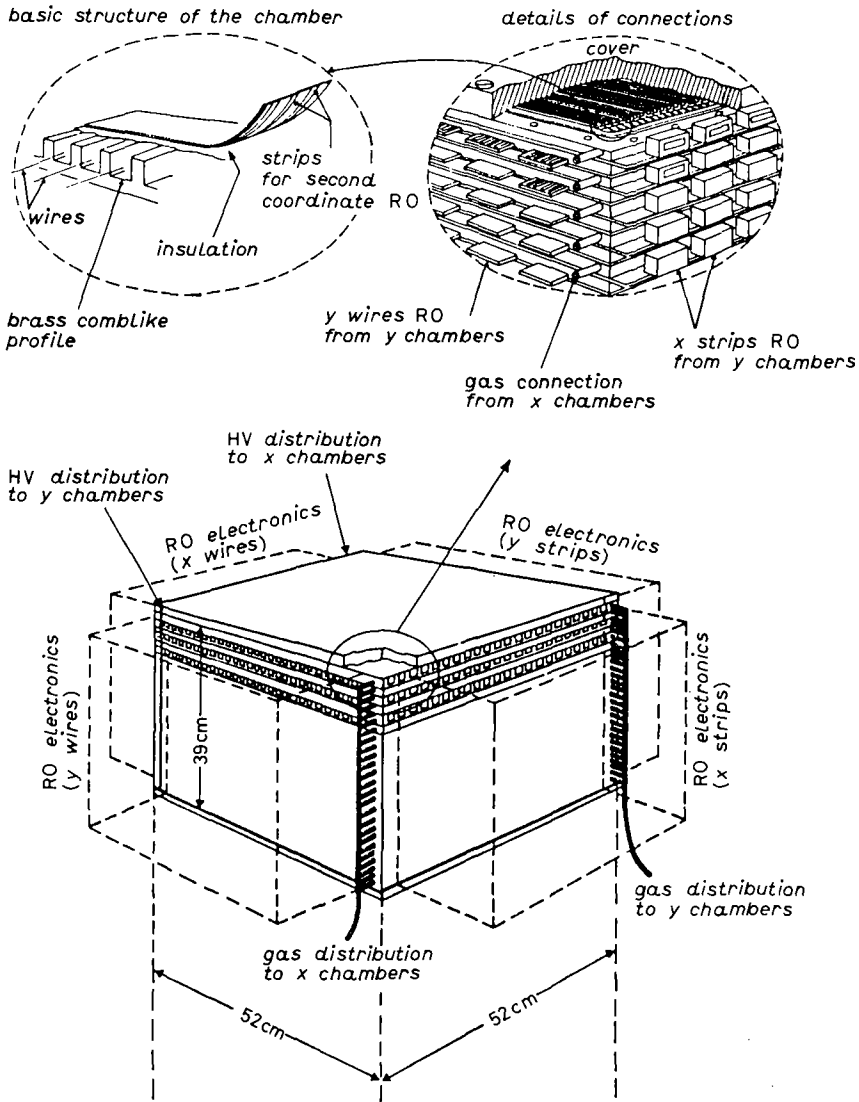

Fig. 2. – Schematic view of the tracking calorimeter.

The calorimeter, shown in fig. 2, is a box of $(52 \times 52 \times 39)$ cm^3 containing 50 planes made of 64 brass tubes; each tube is 8 mm large, 52 cm long, 6 mm high with an internal size of (6.5×5) mm^2 and is equipped with a gold-plated tungsten wire whose diameter is 50 μm. The tubes operate in the streamer mode with isobutane or CO_2. Orthogonal to each tube plane 64 strips (each 52 cm long) are

placed to perform the readout of the induced signal coming from the wire. Every plane (tubes + strips) is rotated with respect to the adjacent ones by 90°, so that not only each plane gives two x, y coordinates, but all along the calorimeter the two coordinates can be obtained also using only tubes or only strips.

The high granularity of the calorimeter comes from the number of readout points (6400), which gives the possibility of reconstructing tracks with good accuracy even if one or more tubes do not work.

The choice of brass tubes (instead of plastic tubes interleaved with an absorber material) was made in order to assure at the same time the absorber-converter function and the detecting function; the absence of passive layers results either in the increase of the number of readout points or in reaching the maximum of compactness in the vertical direction, thus preserving the geometrical acceptance of the whole spectrometer. The brass is a good compromise between compactness and total absorption requirements, to reconstruct the vertex and to contain also the neutral products ($\pi^0 \rightarrow \gamma + \gamma$) of the $\bar{p}p$ annihilation. Table I shows the different volumes of absorber materials and the corresponding weight for a cubic calorimeter to absorb $\pi^0(20\,\lambda_{rad})$, to have a $\pi^{\pm}$ interaction ($2\,\lambda_{int}$) and to stop by range π^+ and $\pi^-(2\langle range \rangle$ at the indicated kinetic energies).

The dimensions and the weight ($\sim 450\,kg$) of the calorimeter are fixed by the boundary conditions (total weight that can be carried in a balloon flight and dimensions of the gondola), and they look as the best compromise to search for antiprotons in a range of few hundreds MeV to several GeV.

For each hit wire (or strip) a 16-bit word is set and, when a signal greater than

TABLE I. – *Dimensions of the calorimeter for different materials.*

	PVC $\rho = 1.3\,g/cm^3$		Cu $\rho = 8.96\,g/cm^3$		Pb $\rho = 11.35\,g/cm^3$	
	side (m)	weight (t)	side (m)	weight (t)	side (m)	weight (t)
π^0 absorption $20\langle\lambda_{rad}\rangle$	10.98	1720.0	0.36	0.42	0.14	0.03
$\pi^{\pm}$ interaction $2\langle\lambda_{int}\rangle$	2.19	13.65	0.38	0.49	0.43	0.90
Stop for range $E_{\pi} = 300\,MeV$ $2\langle range \rangle$	1.22	2.36	0.21	0.08	0.242	0.12
$E_{\pi} = 400\,MeV$ $2\langle range \rangle$	2.31	16.02	0.48	0.99	0.54	1.79
$E_{\pi} = 500\,MeV$ $2\langle range \rangle$	3.78	70.21	0.61	2.03	0.69	3.73

a fixed threshold is achieved, the event pattern is given by the word configuration. For each half plane (32 channels) an analogic signal is provided proportionally to the number of fired wires; these signals can be used for fast trigger combination to reduce on-line the number of events to fulfill the telemetry constraints. The analogic signals can also be used to organize an «intelligent» trigger to pre-select a requested configuration.

3. – The test of a simplified prototype.

A simple prototype consisting of only 24 planes made of small-size brass tubes $(3.5 \times 4.5\,mm)$, operating in the streamer mode, was built for testing. Each plane was interleaved with brass absorbers, 6 mm thick, to stop the incident antiprotons in the middle of the calorimeter. The brass tubes had a comb-like profile covered by a graphited PVC sheet to form an 8-tube module. Each tube was 50 cm long with a gold-plated tungsten anode wire, 50 μm in diameter, held by spacers placed every 15 cm along the tube axis. Each plane was formed by 10 modules, for a total of 80 tubes, giving 1920 readout channels for the whole prototype.

The prototype has been tested at the $T11$ beam line of the CERN proton synchrotron; the beam momentum was adjustable between 0.5 and 3.5 GeV/c with momentum resolution $\Delta p/p \sim 1\%$. In this momentum range the beam (positive or negative on request) consisted of protons, pions, muons, electrons ($\sim 10\%$), kaons ($\sim 1\%$) and, as required, antiprotons ($< 1\%$) following the choice of the polarity. Particle identification was performed, at trigger level, by time of flight (t.o.f), the path for the t.o.f. being 12 m (fig. 3). A t.o.f. window ($\sim 5\,ns$), around the expected peak of the antiproton with momentum of 1 GeV/c was selected and checked with protons of same momentum. About 200 antiproton
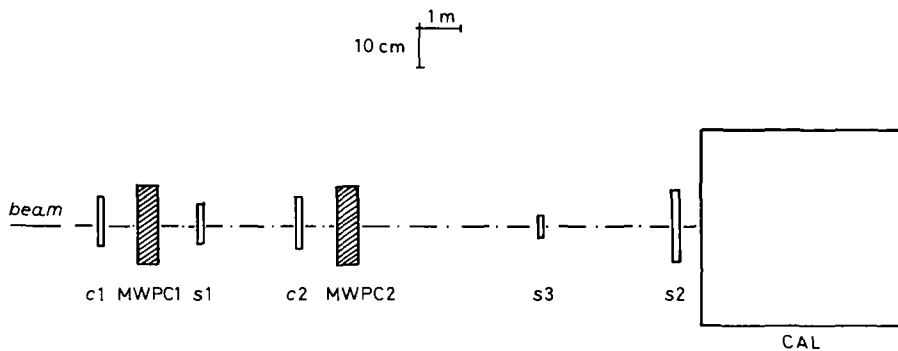

Fig. 3. – Set-up for the test at CERN PS: $c1$, $c2$: Čerenkov counters. MWPC1, MWPC2: multiwire proportional chambers for beam position monitoring. $s1$, $s2$, $s3$: photomultipliers for t.o.f. CAL: calorimeter. Beam: $2 \cdot 10^{11}$ particles/pulse, π^-: $\sim 4 \cdot 10^5$, $\bar{p}$: $5 \cdot 10^3$, e^-: 10% and μ: $\sim 10^5$.

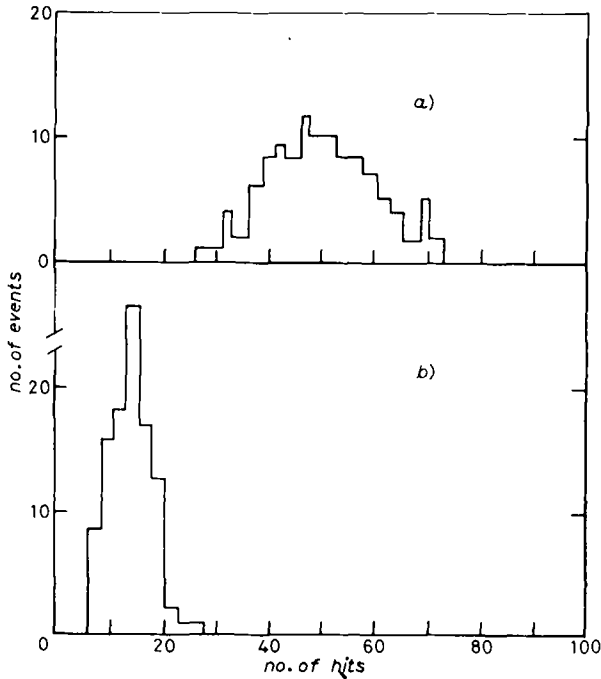Fig. 4. – Event distribution as a function of the number of hit tubes (proportional to the released energy) for a) antiprotons, b) protons both at 1 GeV/c momentum.

candidates were collected during several runs. Chamber alignment and geometry was controlled by exposing the calorimeter to muons.

This calorimeter prototype has shown to be able to detect and identify antiprotons by

a) total released energy,

b) vertex identification combined with an annihilation star topology.

The released energy of the interacting hadrons is related to the number of streamer tubes fired in the event; this value for 1 GeV/c antiprotons, as shown in fig. 4 is, on the average, 4 times higher than for a proton of the same momentum. The event distribution, at 1 GeV/c, for $\bar{p}$ candidates and for negative particles contained in the beam (π^-, K^-, e^-) is shown in fig. 5.

A detailed study of the event configuration showed that 80% of the antiproton candidates had an interaction vertex with 3 or more prongs as expected for $\bar{p}$-p annihilation. The rest of the candidates ($\sim$ 20%) had no clear pattern due either to a nontotal containment (incident track out of the geometry) or to the absence of a second readout coordinate (y) for the tracks to solve ambiguities. This problem will be partially overcome in the present full-scale calorimeter where the second coordinate, provided by the strips, is available.
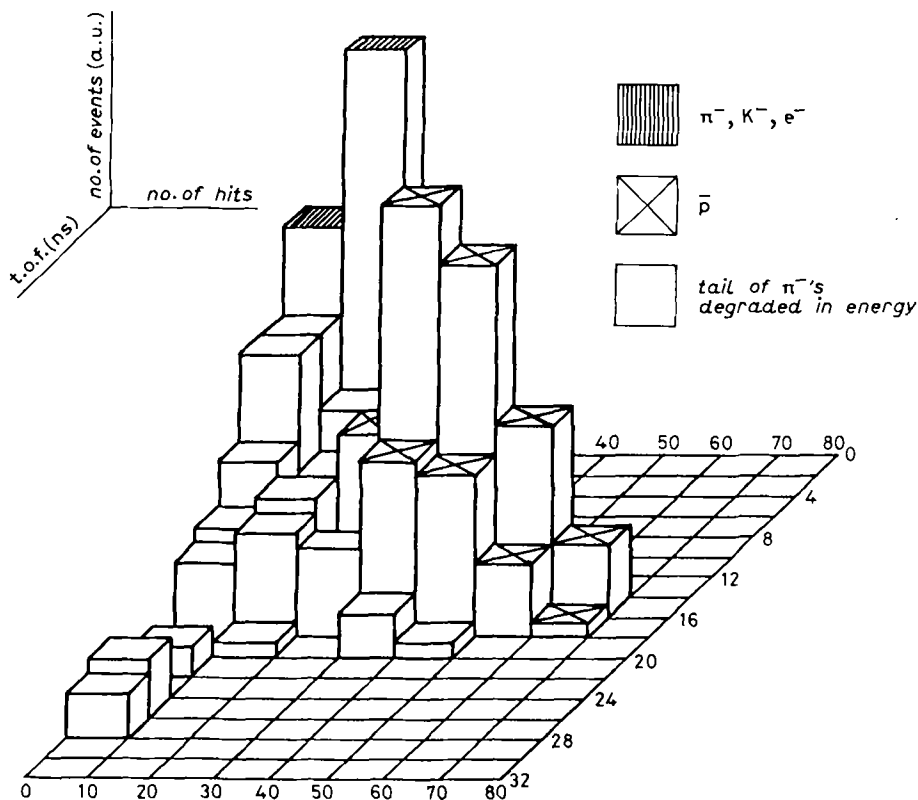
Fig. 5. – Event distribution as a function of the number of hit tubes and of the time of flight windows. Events in the low edge of the plot are 1 GeV/c negative pions, kaons and electrons, while events clustering in the narrow t.o.f. window of ~ 6 ns exhibit a released energy compatible with that of antiprotons of 1 GeV/c momentum. The remaining events are to be considered as the background mainly due to pions.

4. – Fast, low-power readout electronics.

The electronic readout of the calorimeter is accomplished by a 32-channel card constituted by three main functional blocks. A special effort, in the card design, was devoted to preserve compactness and low-power consumption; in fact, the allocation of the front-end electronics has been carried out with the choice of hybrid circuit technology which allows to fix high-density printed circuit boards on both sides of each streamer tube plane; furthermore, a value of power dissipation of 15 mW/channel has been obtained mantaining at the same time a good stability in the amplification gain which is better than 0.2% per °C. Before digitization, signals coming from wires and strips are preamplified following the scheme shown in fig. 6; due to the fact that the induced signals on the strips are ~ 3 times lower than the corresponding signals on the wires, the circuit shown in
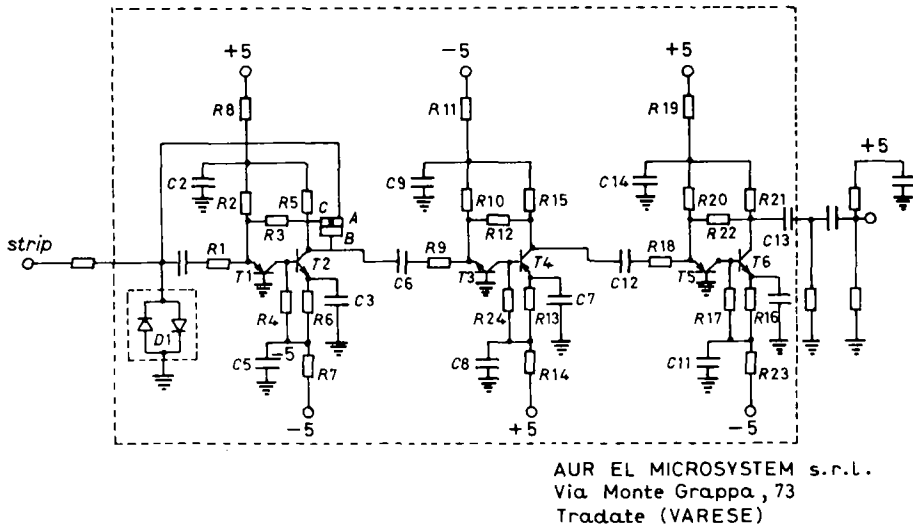
AUR EL MICROSYSTEM s.r.l.
Via Monte Grappa, 73
Tradate (VARESE)

Fig. 6. – The preamplifier circuit of the readout system.

fig. 6 is provided with one more amplification stage (the third one, close to the output) for the strips in respect to the one for wires. One of the main parameters defining the features of such electronics is the sensitivity of the amplification threshold per each channel: the chosen values, 0.5 pC for wires and 0.2 pC for strips, are well below the minimum typical values of the collected charge (~ 2 pC on wires for 20 ns collection time).

All the functions necessary to generate the same status flags to the remote digital electronics are accomplished by a sequential chain of CMOS shift registers which perform the temporary storage of the status of all wires and strips still inside the calorimeter.

Furthermore, for each group of 32 channels an analog signal is read out, with a value proportional to the number of hitting wires inside the group itself. This analog readout allows the external trigger to generate a storage command for the shift registers; the acquisition of the digital information stored inside the calorimeter is performed by four C.A.E.N. STAS (streamer tube acquisition system) controllers; each one provides the calorimeter with a readout rate of 1.25 Mbits/s per channel and offers the possibility to read out in serial mode the calorimeter and to transmit the information to a standard CAMAC interface.

5. – The complete apparatus.

The calorimeter described in this paper is a part of an apparatus composed by a magnetic spectrometer built by the New Mexico State University [18] with two

[18] R. L. GOLDEN, G. D. BADHWAR, J. L. LACY and J. E. ZIPSE: Nucl. Instrum. Methods, 148, 179 (1978).

plastic scintillators at the top and the bottom for time-of-flight measurements.

The magnetic spectrometer is made by a superconducting magnet (61 cm in diamater, weight 150 kg) producing a magnetic field of 40 kG (at a current of 120 A) and a stack of 8 multiwire proportional chambers (MWPC). The rigidity limit is $R \leqslant 200$ GV and the power consumption is ~ 700 W.

Each MWPC has dimensions of (50×50) cm^2 and provides a spatial resolution of ~ 200 μm r.m.s. To follow the development of the incoming tracks, the position
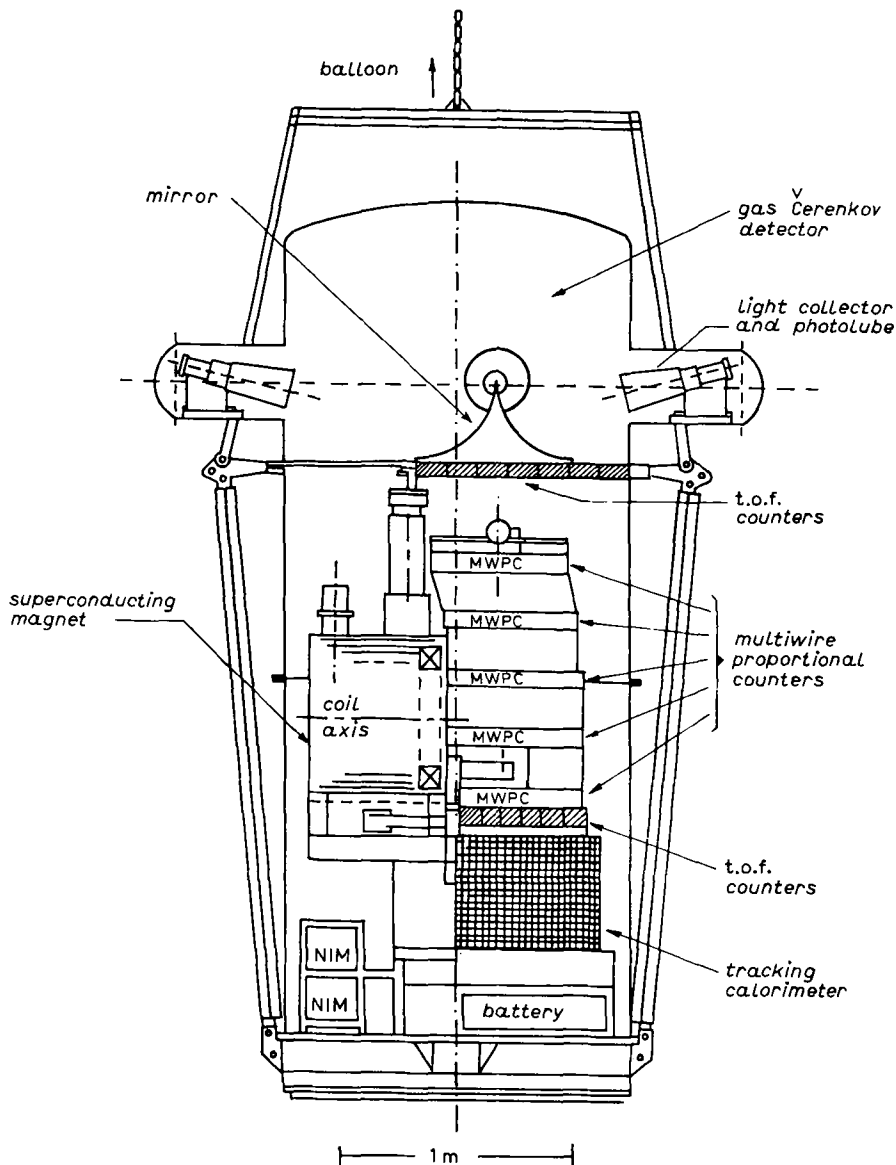

Fig. 7. – The apparatus placed in the gondola for the balloon flight.

measurement in both cathode and anode wires is obtained by measuring the time of arrival of the signal at each end of the delay lines coupled to the wires themselves.

A gas Čerenkov counter is located above the spectrometer and can be filled with air (for the detection of electrons and positrons) or with sulfur hexafluoride (to discriminate antiprotons); its aperture is divided by four spherical mirrors viewed each by a 12.5 cm 4525 RCA phototube. The effective path length of the detector is 80 cm and its efficiency in detecting fully relativistic electrons is 65% for the first configuration and more than 92% in discriminating $\bar{p}$'s (reducing the muon contamination to less than 10% of $\bar{p}$).

The calorimeter covers the same area of the MWPCs and is very compact, so that the geometric acceptance (400 cm^{2}sr) does not decrease.

The whole apparatus, as shown in fig. 7, is contained in a gondola, 5 m high, which is able to transport 3 tons, and will be carried by a balloon at an altitude of ~ 40 km in a Canadian region, as close as possible to the magnetic North Pole, to reduce the geomagnetic cut-off.

The control of the apparatus in flight is performed with CAMAC and NIM electronics either in the payload or at ground and it is possible to select various trigger configuration counters by radio commands, as well as to switch off every device independently. The digitized data are transmitted to the ground with a 156 kbit/s telemetry link which provides a maximum event rate of 290/s. Every information concerning the status of the various operations (temperatures, voltages, pressures etc.) is also transmitted.

This apparatus has been designed to be one of the most powerful detector to study specifically cosmic e$^+$ and e$^-$, p, $\bar{p}$ antihelium and helium nuclei within the limits of the flight boundary conditions, providing a very good t.o.f. resolution, momentum and energy measurements, pattern reconstruction, with high geometric acceptance.

6. – Conclusions.

A calorimeter suited for the detection of antiprotons in space experiments should fulfil the following major requirements:

1) full containment of the annihilation event in the energy range of interest;

2) good vertex reconstruction of the annihilation star;

2) compactness;

4) high mechanical stability and reliability;

5) good energy resolution.

The calorimeter we built satisfies such requirements and is expected in conjuction with the spectrometer to detect clearly positrons and antiprotons in space.

● RIASSUNTO

Un calorimetro tracciante costituito da cinquanta piani realizzati con 3200 tubi a streamer in ottone accoppiati ad un egual numero di strip per la raccolta del segnale indotto, è uno strumento ideale per operare in connessione con uno spettrometro magnetico, allo scopo di rilevare antiprotoni cosmici. Si presentano le caratteristiche di tale calorimetro, i risultati del test preliminare di un prototipo e le proprietà dell'intero apparato. L'apparato stesso, progettato per essere trasportato da un pallone ad una quota di circa 40 km, può essere considerato come un rivelatore di seconda generazione, capace in linea di principio di risolvere la questione ancora aperta, a causa del disaccordo tra i dati sperimentali esistenti, della presenza nei raggi cosmici di antiprotoni di bassa energia ($\leqslant 1\,\mathrm{GeV/c}$).

Калориметр, связанный с магнитным спектрометром, для летектирования первичных космических антипротонов.

Резюме (*). — Трековый калориметр, состоящий из 3200 латунных стримерных трубок, связанных с 3200 чувствительных лент, дополняется магнитным спектрометром для детектирования первичных космических протонов. Представляются характеристики такого калориметра, результаты предварительных испытаний прототипа калориметра, а также свойства всей аппаратуры в целом. Предложенная аппаратура, которая будет действовать на воздушном шаре на высоте порядка 40 Km, может рассматриваться как второе поколение детекторов, способных, в принципе, решить проблему обнаружения антипротонов низких энергий ($\leqslant 1\,\text{ГэВ/c}$) в космических лучах, которая до сих пор остается открытой из-за несоответствия существующих экспериментальных данных.

(*) *Переведено редакцией.*